PHOTONIC LATTICES AS DIFFRACTION BASED CHEMICAL SENSORS

Ryan C. Bailey, Biing-Chiau Tzeng, Xiaojun Dang, Gary A. Mines, Keith A. Walters, and Joseph T. Hupp
Dept. of Chemistry, Materials Research Center, and Institute for Environmental Catalysis, Northwestern University, 2145 Sheridan Road, Evanston, IL 60208 USA

A new approach to chemical sensing based upon the modulation of coherent visible light by chemoresponsive photonic lattices is presented. Sensors are designed so that they produce a diffraction pattern which reports on the local environment of the lattice. Changes in the "diffraction efficiency" of a lattice induced by interaction with a volatile or condensed-phase analyte provides the sensing modality. The methodology presented is potentially universal since all atomic and molecular analytes possess polarizable electrons, and thus have refractive indices greater than vacuum. Most are greater than water, allowing for aqueous sensing. An extension on initial investigations is also presented which utilizes resonance enhancement effects to increase device sensitivity and possibly offer analyte selectivity.

INTRODUCTION

We wish to describe a new approach to chemical sensing that is chemically general, inexpensive, and conceptually straightforward. The approach is based on the interaction of coherent light (for example, the output of a low-cost laser pointer) with a chemoresponsive lattice featuring periodic microscale spacing. As shown below, in its initial incarnation the approach has reasonable absolute sensitivity when used under "off resonance" (non-light-absorbing) conditions. When implemented under resonance conditions, it becomes significantly more sensitive and potentially more selective. While not developed here, the technique clearly can be implemented in an array motif, and clearly can be extended to biological sensing, including whole cell sensing.(*1*) Finally, as we have shown elsewhere, variants of the technique can be usefully applied to other problems, including: a) monitoring molecular adsorption at electrode/solution interfaces,(*2*) and b) determining conduction-band-edge energies for nanocrystalline semiconductor electrodes.(*3*)

CONCEPTUAL BACKGROUND

Any periodic pattern featuring alternating regions of high and low refractive index is capable of diffracting electromagnetic radiation of wavelength comparable to the pattern element spacing. If the incident radiation is coherent and monochromatic, interaction with the pattern or grating will generate a characteristic diffraction pattern that is related to the physical pattern via an Fourier transform. The diffraction efficiency, DE, depends on the lattice thickness or optical pathlength, d, and the difference in refractive index, Δn, between the high and low n regions. (DE is operationally defined here as the ratio of the intensity of diffracted light to total transmitted light intensity.) In the short pathlength limit, for a one-dimensional grating featuring sinusoidal periodicity, the first-order diffraction efficiency is well described by eq. 1:

$$DE = [\pi \Delta n d/\lambda]^{1/2} \qquad [1]$$

where d is the lattice thickness (optical pathlength) and λ is the wavelength of incident light.(*4*) As we will show elsewhere, however, the relation can become considerably more complex - leading to both positive and negative responses - if the optical pathlength is long or if the index difference (contrast) is extraordinarily large.

Given the sensitivity of the diffraction response to even small changes in refractive-index contrast, we reasoned that any recognition, binding, or uptake event that selectively altered the index in only one of the two sets of periodic segments comprising the lattice could be detected as a *change* in diffraction efficiency. Scheme 1 illustrates the concept and shows why the method is a universal sensing scheme. Briefly, for the case shown, the contrast medium is air (essentially vacuum, $n_1 = 1$) and the lattice material is a porous, high-internal-surface-area material capable of selectively binding or adsorbing from the vapor phase a volatile target compound. Before binding, the refractive index (n_2) in the porous lattice region is a volume-weighted composite of refractive indices for the lattice material itself ($n > 1$) and vacuum ($n = 1$). Porous-lattice adsorption of any molecule obviously will fill some of the vacuum region. This, in turn, will increase the weighted-composite refractive index (n_2'), increase the index contrast (Δn), and increase the diffraction efficiency (eq. 1). In contrast to sensing based on properties such as luminescence, visible-light absorption, or well-defined redox reactivity, *sensing based on diffractive photonic lattice responses is, in principle, chemically universal* since all molecular compounds possess refractive indices greater than 1 (greater than vacuum). (Recall that the refractive index is a measure of the interaction of polarizable electrons with electromagnetic radiation, and that all electrons - even core electrons - are to some degree polarizable.)

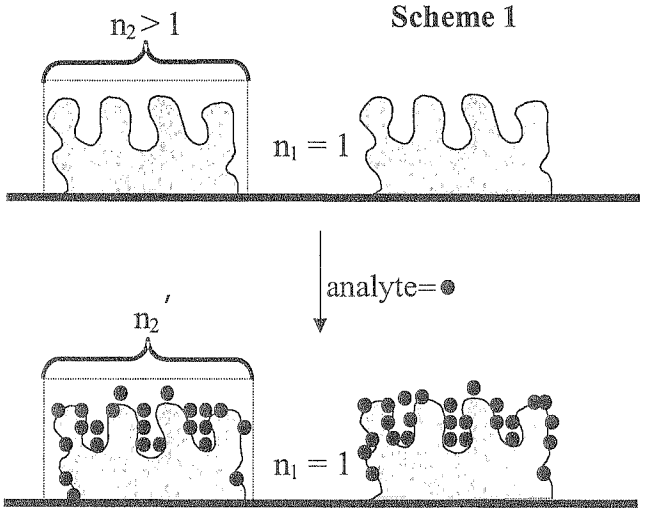

EXPERIMENTAL DESIGN

Photonic-lattice based sensor construction relies upon the fabrication of a micro-patterned thin film ("lattice") of a chemoresponsive material on a transparent platform such as glass. (In principle, semi-transparent platforms or reflective platforms also could be used.) For many candidate lattice materials, micropatterning can be readily accomplished by using one of several "soft lithography" techniques (microcontact printing, micro-transfer molding, micro-molding in capillaries, etc.) developed and popularized by Whitesides and co-workers.(*5*) The applicability of Whitesides' techniques is remarkably broad; in our own lab we have successfully fabricated efficiently diffracting lattices composed of mesoporous molecular materials, charge-transfer salts, wide bandgap semiconductors,(*2, 3, 6*) metal nanoparticles,(*7*) conducting polymers,(*8*) dielectric polymers, and self-assembled monolayers. Figure 1 shows a low-resolution atomic force micrograph of representative thin-film photonic lattice composed of a vapochromic charge-transfer salt.

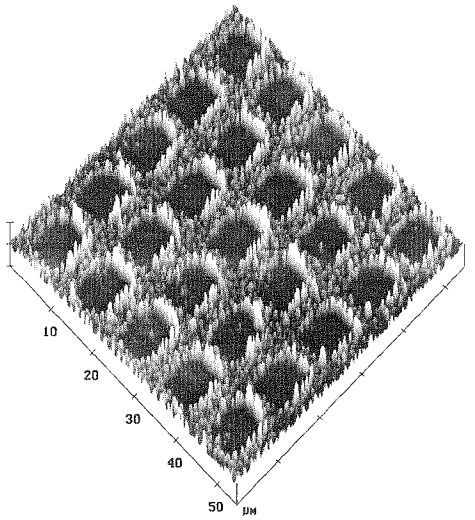

Figure 1. 55 x 55 μm TM-AFM image of a representative photonic lattice. The lattice material is a vapochromic charge-transfer salt.

Figure 2 shows the diffraction pattern generated by a square lattice like that in Figure 1. The light source is an attenuated low-power He-Ne laser and the pattern is easily visible to the naked eye. In the figure, the bright center spot corresponds to undiffracted light; closest to this point are spots due to first-order diffraction in the x-direction, y-direction, or both. Also readily observable experimentally are a large number of spots due to higher-order diffraction. For the lattice, the magnitude the diffraction efficiency, as noted above, depends on the degree of refractive index contrast between the patterned material and the surrounding medium (typically, water or air). If the diffracting material absorbs a contaminant from the surrounding medium, its refractive index will change (typically, it increases) and the diffraction efficiency will change (again, it will usually increase). DE can be evaluated in real time using a pair of low-cost photodiodes – one collecting diffracted light and one collecting residual undiffracted light; Scheme 2.

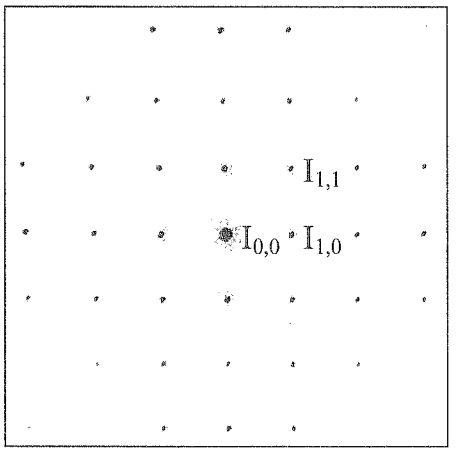

Figure 2. Typical optical diffraction pattern from 2-D chemoresponsive photonic lattice.

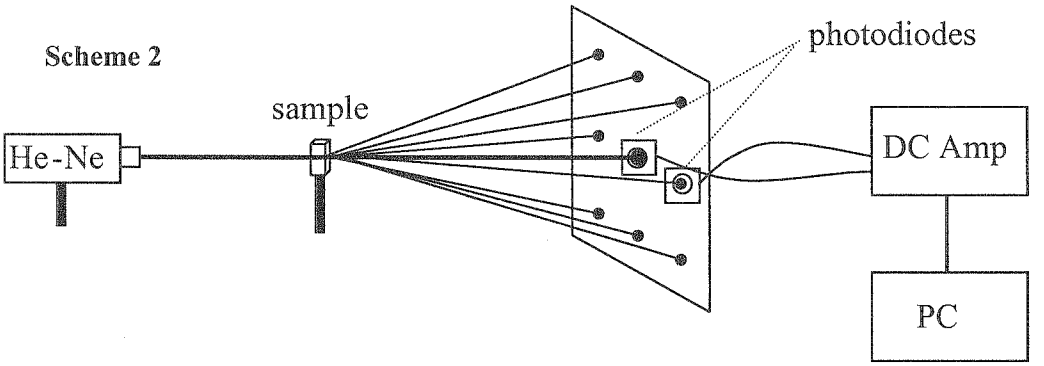

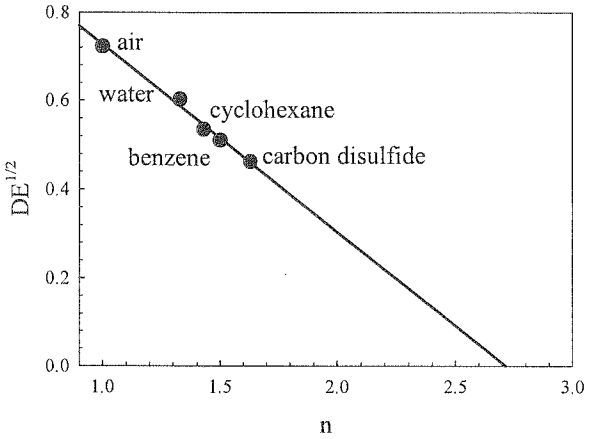

Figure 3. Square root of diffraction efficiency versus refractive index of surrounding medium for a patterned anatase film in contact with air or with various solvents. The x-intercept of the best-fit straight line (i.e. complete index matching) corresponds to the refractive index of anatase.

Figure 3, adapted from reference 2 illustrates the dependence of DE on the magnitude of the refractive-index contrast between the lattice and its surroundings. Charted is the square root of diffraction efficiency versus n (see eq. 1) for an inverse lattice composed of high-porosity TiO_2 (anatase) in contact with air or solvent. High contrast combinations yield efficient diffraction, while lower contrast combinations diffract less efficiently. Extrapolation of the plot to DE = 0 (perfect solvent/lattice index matching) yields the refractive index of the lattice material itself. The value obtained (2.72) is very close to the literature value for the rutile form of TiO_2.(*9*)

REPRESENTATIVE APPLICATIONS

Volatile organic chemical sensing. As a first step toward organic chemical contaminant sensing, we have carried out pilot experiments based on micropatterned lattices composed of poly(4-vinylphenol). We reasoned that the polymer would show modest chemical selectivity, favoring hydrophilic compounds over hydrophobic compounds. Because of the greater experimental simplicity of vapor-phase studies, initial experiments involved sensing of candidate contaminants as pure vapor-phase compounds. Figure 4 shows the response of a lattice to

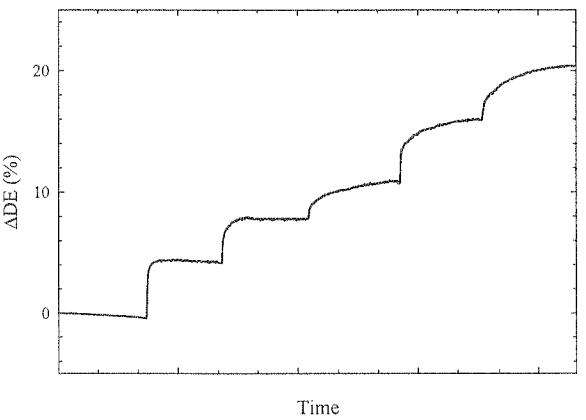

Figure 4. Diffraction-based observation of methanol uptake by a micropatterned thin film of poly(4-vinylphenol) Arrows indicate points in time where aliquots of methanol vapor were added.

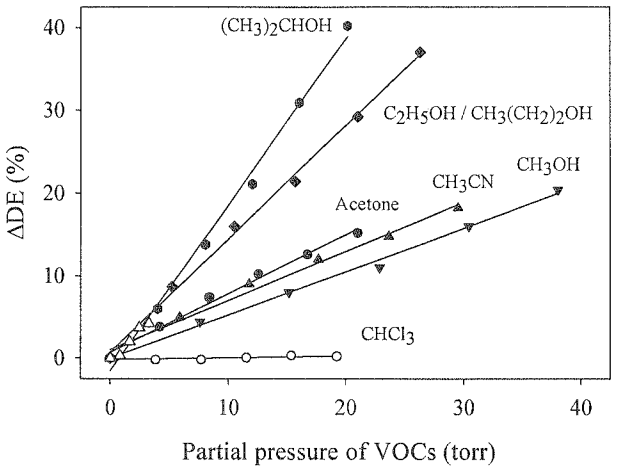

Figure 5. Change in diffraction efficiency versus vapor pressure of volatile organic chemical, for several VOCs. Lattice is composed of poly(4-vinylphenol). Probe wavelength is 633 nm.

increasing amounts of methanol. Figure 5 summarizes the response of the lattice to several volatile organic compounds (VOCs). Comparatively large responses are seen from alcohols and other polar compounds, but almost no response is seen from chloroform. The lattice similarly discriminates against other low polarity compounds like n-hexane (data not shown). For the VOCs that are sensed, linear correlations exist between sensor signal (change in diffraction efficiency) and VOC vapor pressure.

Similar results have been obtained by using a photonic lattice composed of a porphyrinic molecular square compound(*10*) and prepared via a variant of the "micro-molding in capillaries" technique. The material, which contains cavities of ca. 2 nm width, features an enormous void volume and a substantial internal surface area. As will be described elsewhere, the photonic lattice response was benchmarked against the response obtained by quartz crystal microgravimetry for each of three VOCs. Quantitative agreement was obtained. The comparison also provided information relevant to detection limits. Uptake of a few nanograms of analyte proved detectable with a pattern a few square millimeters in area. For comparison, high-quality QCM instruments are capable of sensing the uptake of about 0.5 ng of analyte material. We believe that significantly better sensitivity can eventually be achieved in the photonic lattice experiment by employing a mode-stabilized power source and by implementing lock-in techniques.

Resonance enhanced diffraction and sensing. In the examples described above, sensing is based on changes in diffraction efficiency deriving from changes in the real component of the refractive index far from any absorption band. The refractive index of any material, however, is much different at wavelengths where the material absorbs light ("resonance") than where it does not absorb light ("off resonance"). The connection between the real component of the refractive index and absorptivity is given by the Kramers-Kronig relation:

$$\Delta n(\omega') = \frac{c}{\lambda} \int_0^\infty \frac{\Delta\alpha(\omega)}{\omega^2 - \omega'^2} d\omega \qquad [2]$$

where $\Delta\alpha$ is the change in absorptivity and ω' is the optical frequency of interest (*11*). Figure 6 illustrates the relationship for two simple Gaussian absorption profiles. Particularly compelling are the sharp changes in index near the absorption maxima. If analyte binding induced an increase or decrease in lattice absorptivity (for example, via

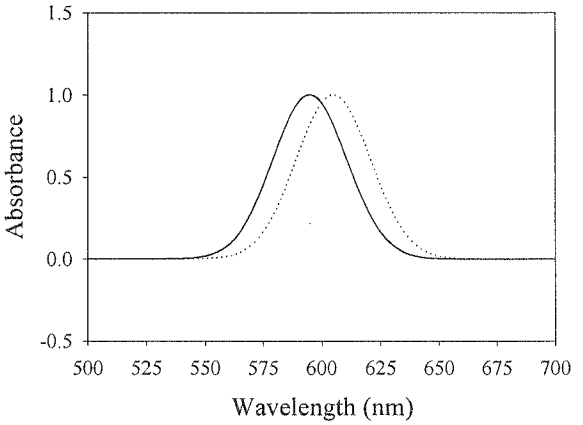

Figure 6. Simulated red shift in a Gaussian absorption profile resulting from analyte binding event.

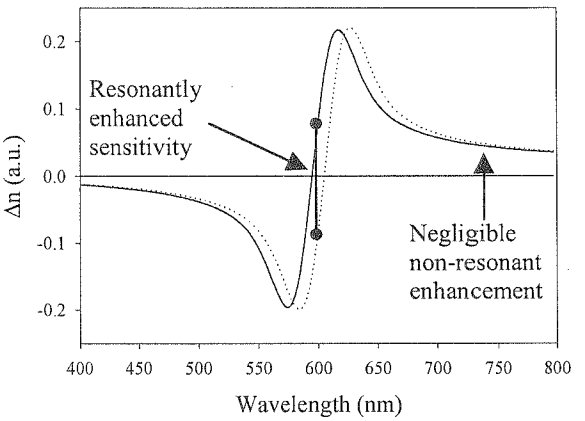

Figure 7. Results of Kramers-Kronig analysis on the simulated Gaussian absorption profiles in Figure 6. Note the sharp changes in refractive index proximal to the absorption maxima.

lattice/guest-molecule charge-transfer interactions), a much larger change in refractive index would be expected for measurements made at resonant wavelengths than at non-resonant wavelengths - and, therefore, a much larger change in diffraction efficiency. Even more striking could be measurements made near the lattice absorption maximum under conditions where target-molecule uptake induces a wavelength shift in the maximum. A comparison of the dotted and solid curves in Figure 7 illustrates the extreme sensitivity of the refractive index, and therefore, the diffraction efficiency, to such spectral shifts. In principle, advantage could be taken of these resonance effects to amplify diffraction efficiency changes and extend lattice sensitivity.

As a proof-of-concept, we examined chloroform sensing by photonic lattices of the "vapochromic" charge transfer salt, $[Pt(CNC_6H_4C_{10}H_{21})_4][Pd(CN)_4]$.(*12*) Uptake of chloroform vapor induces a limiting shift in the compound's charge-transfer absorption maximum from 570 nm to 600 nm. A Kramers-Kronig analysis predicts maximum resonant amplification at 640 nm, significant amplification at 525 nm, no amplification at 538 nm and 619 nm (the wavelengths where the sign of the imaginary contribution to the complex refractive index change), and significant *de*amplification at 583 nm. The magnitudes of the amplification and attenuation effects can be predicted only

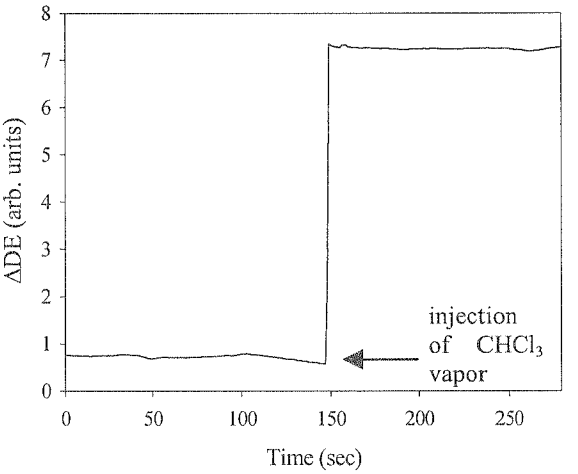

Figure 8. Detection of chloroform as monitored by a vapochromic photonic lattice. Arrow marks time of vapor injection. Rapid uptake and signal transduction lead to extremely fast sensor response. A 50-point floating average was implemented before and after the injection to remove higher frequency laser fluctuations.

if lattice absorptivities are known; in this case they are not. Experimental measurements show, however, that uptake is nearly undetectable at λ =583 nm, even under isotherm-saturation conditions. At λ = 633 nm, however, very substantial amplification is evident and concentrations of chloroform as low as 4 μM are easily sensed, as shown in Figure 8. Signal-to-noise considerations, even at this stage, suggest a detection limit on the order of 100 nM. For comparison, all sensing demonstrations to date of the charge-transfer salt to date have been carried out in an analyte-saturated environment.

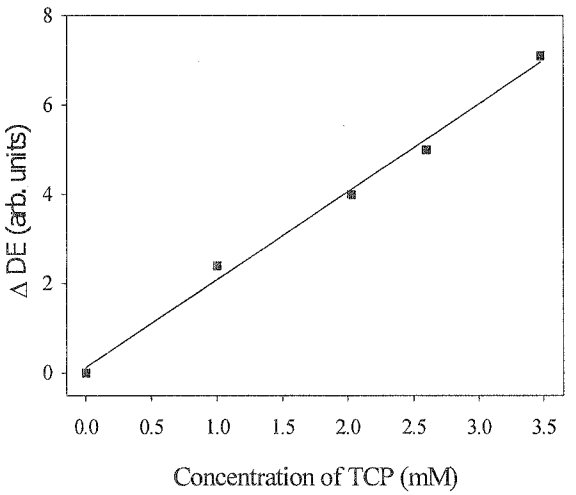

Figure 9. Plot of diffraction efficiency vs. concentration of 2,4,5-trichlorophenol in an aqueous solution. The photonic lattice material used was poly(4-vinylphenol).

Aqueous-phase contaminant sensing. What about sensing in aqueous environments? The prospects for nearly universal sensing here are also very good because water possesses an anomalously low index (n = 1.33) that provides contrast to almost all other substances. For example, under non-resonance conditions most organic compounds, including biological compounds such as proteins and oligonucleotides, possess refractive indices between 1.4 and 1.5. Figure 9 summarizes the results of a preliminary extension of the experiment in Figure 5 to an aqueous environment. As illustrated in the figure, the lattice-based sensor responds approximately linearly to 2,4,5-trichlorophenol as a contaminant in water.

A second example involves metal-ion uptake. Scheme 3 illustrates the binding of a metal ion by a diimine receptor site along a chromophoric polymer chain. As suggested by the scheme, binding can be reversed by exposing the polymer to an extraction agent

Scheme 3

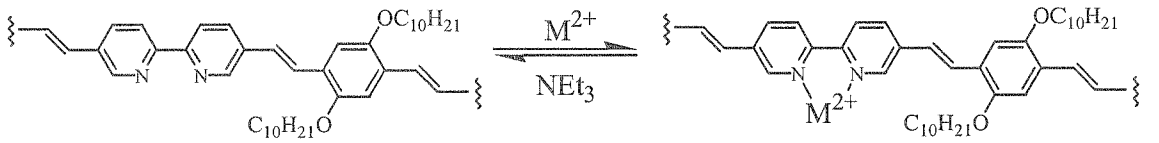

having an even higher affinity for the metal ion - a concept that Wasielewski and co-workers (the designers of the polymer) have successfully experimentally documented.(*13*) This, in turn, should permit re-use of the sensor. We have prepared micropatterned lattices of the diimine polymer and evaluated the lattices as sensors for zinc ions. Our rationale in using the polymer for diffraction based sensing

was that we could amplify signals (i.e. changes in DE) by taking advantage of resonance enhancement effects. As suggested by the data in Figure 10, resonance effects come into play because metal ion uptake causes a shift in absorbance to longer wavelength. (Because the receptor-functionalized phenylenevinylene is not swollen by pure water, experiments were run in water/ethanol mixtures. As shown in Figure 11, zinc ion uptake at millimolar levels is easily observed by monitoring DE. Figure 11 additionally shows that the sensor response is reversible based on triethylamine extraction of the incorporated zinc ion.

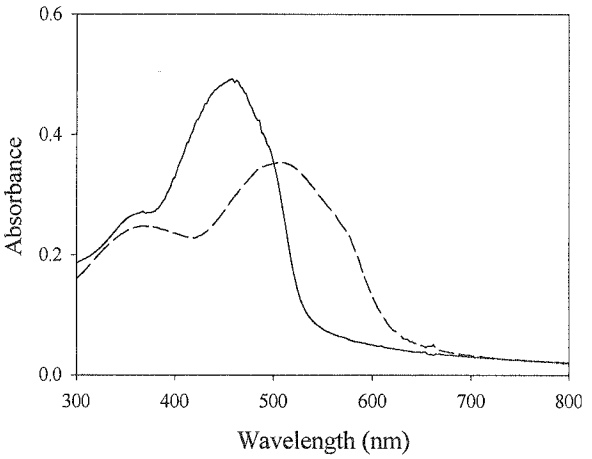

Figure 10. Absorption spectra of the diimine polymer system (20:80 H_2O:EtOH) before (solid line) and after (dotted line) exposure to Zn^{+2}.

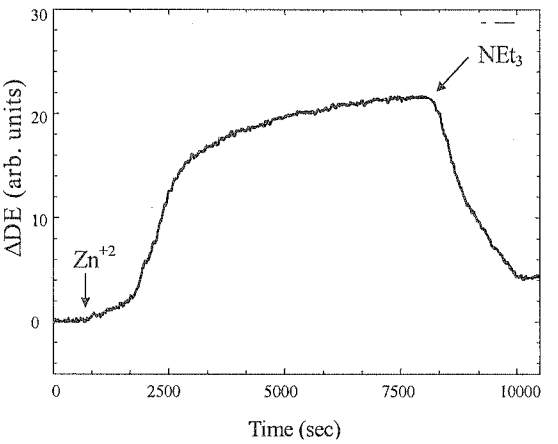

Figure 11. Real-time observation of Zn^{+2} uptake by diimine polymer as detected by a photonic lattice sensor.(20:80 H_2O:EtOH)

Figure 12 shows the outcome of a computational prediction of the change in refractive index, Δn, as a function of probe-light color (wavelength). The input for the simulation - a Kramers-Kronig transformation - was the linear spectral data shown in Figure 10. From the simulation, certain probe wavelengths should yield positive signals in response to zinc ion uptake, others should yield negative signals (decreases in diffraction efficiency), while still others should yield no signal. Because the absorption spectral changes induced by other metal ions differ from those seen for zinc(*13*) the simulated resonant refractive index changes (Kramers-Kronig plot) likewise will differ.

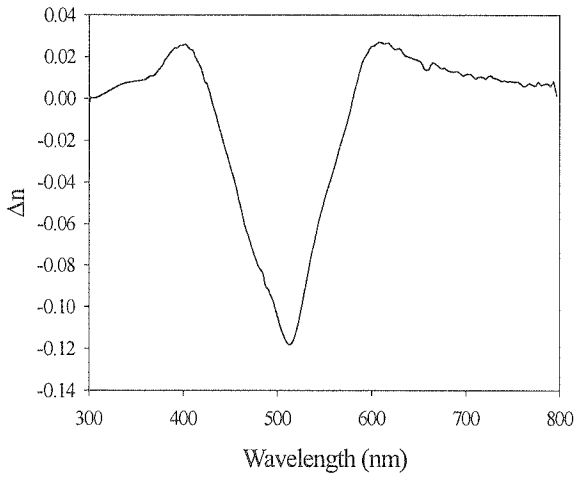

Figure 12. Results of Kramers-Kronig analysis predicting the change in refractive index of the diimine polymer because of Zn^{+2} addition. The absorption spectra shown in Figure 10 were used as the input data.

We suggest that it should be possible to exploit these differences by constructing multi-probe-color experiments that will enable one to determine the chemical identity of the metal ion being sensed or permit one to sense multiple metal ions independently with a single micropatterned polymer film.

Absorption kinetics. Figure 13 shows the *time-resolved* response of a photonic lattice of poly(4-vinylphenol) to several simple VOCs. In principle, the time response can be used to assess *rates* of target molecule absorption (or release). The inexpensive photodiodes used in our existing instrument have sub-100 ns response times, suggesting that very fast processes can be followed. (Indeed, the ultimate limitation on kinetics measurements almost certainly will be the rate at which analytes can be delivered to the sensor, not the response time of the instrument's detection elements.) For comparison, we note that quartz crystal microgravimetry, even when run using dual oscillator schemes, is limited to bandwidths of only a few to several hertz.(*14*)

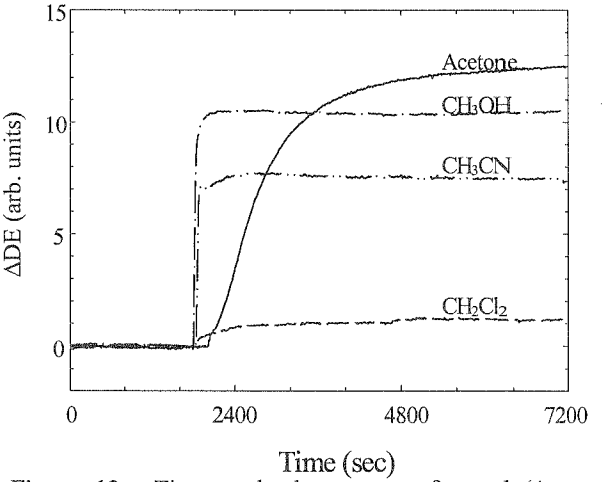

Figure 13. Time-resolved response of a poly(4-vinylphenol) photonic lattice upon exposure to several organic vapors.

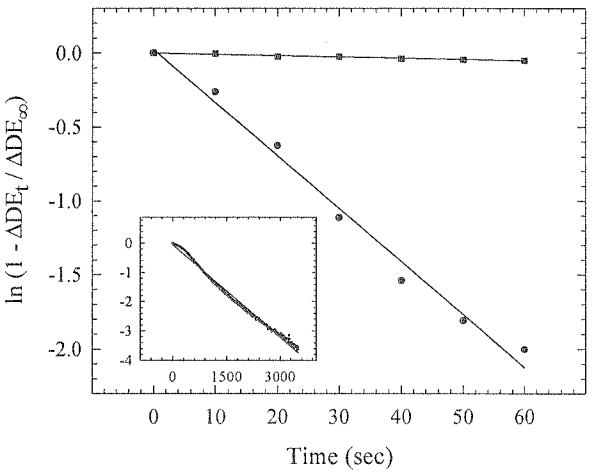

Figure 14. Kinetic analysis of VOC uptake by poly(4-vinylphenol) gratings. ● : Ethanol ($k = 3.6 \times 10^{-2}\ s^{-1}$); ■ : Acetone ($k = 1.1 \times 10^{-3}\ s^{-1}$). Inset plot shows the complete acetone uptake experiment run. Kinetic plots are constructed based on $1-\frac{\Delta DE_t}{\Delta DE_\infty} = \exp(-kt)$, where ΔDE_t is the diffraction efficiency change at time t and ΔDE_∞ is the diffraction efficiency change at the completion of the experiment. It is assumed that the two analytes induce equivalent refractive index changes upon uptake of equivalent amounts in the grating film.

As shown in Figure 13, even for the simple case of poly(4-vinylphenol) remarkably different film absorption kinetics can be observed for similarly sized molecular analytes. A diffusion kinetics analysis, for example, yields a 30-fold larger rate constant for ethanol absorption than for acetone absorption by the phenol lattice; Figure 14 .(*15*) Additional experiments will be required in order to establish whether the diffusion analysis or an alternative analysis is mechanistically more appropriate. It is clear, however, that photonic lattice diffraction measurements can be used to generate the needed kinetic data.

CONCLUSIONS

Chemoresponsive photonic lattices comprise a versatile new class of chemical sensors. The sensors function by recording changes in the efficiency of lattice diffraction of visible coherent light upon uptake of volatile or condensed-phase analytes. In contrast to sensing based on properties such as luminescence, visible-light absorption, or well-defined redox reactivity, *sensing based on diffractive photonic lattice responses is, in principle, chemically universal* since all molecular compounds possess polarizable electrons and therefore have refractive indices greater than vacuum. Most also have indices greater than water. Resonant amplification of the diffraction response offers a basis for enhancing the device sensitivity as well as selectivity.

ACKNOWLEDGMENTS

We thank Prof. Michael Wasielewski for providing a sample of the receptor-functionalized phenylenevinylene polymer used for metal ion sensing. We thank the Water Environment Research Foundation (BCT), the U.S. National Science Foundation (GAM), the Northwestern Materials Research Center (RCB), and the Northwestern Institute for Environmental Catalysis (XD) for financial support of our work.

REFERENCES

1. R. C. Bailey, M. Parsek, and J. T. Hupp, unpublished results.
2. X. Dang, K. J. Stevenson, and J. T. Hupp, *Langmuir,* accepted, (2001).
3. X. Dang, A. M. Massari, and J. T. Hupp, *Electrochem. and Solid State Lett.* **3**, 555 (2000).
4. M. Hasegawa, T. Yamamoto, A. Kanazawa, T. Shiono, and T. Ikeda, *Chem. Mater.* **11**, 2764 (1999).
5. Y. N. Xia and G. M. Whitesides, *Angew. Chem. Int. Ed.* **37**, 551 (1998).
6. K. J. Stevenson, G. J. Hurtt, and J. T. Hupp, *Electrochem. and Solid State Lett.* **2**, 175 (1999).
7. R. C. Bailey, K. J. Stevenson, and J. T. Hupp, *Adv. Mater.* **12**, 1930 (2000).
8. A. M. Massari, K. J. Stevenson, and J. T. Hupp, *J. Electroanal. Chem.* **500**, 185 (2001).
9. J. Carper, The CRC Handbook of Chemistry and Physics, (1999).
10. R. V. Slone and J. T. Hupp, *Inorg. Chem.* **36**, 5422 (1997).
11. K. S. Schanze, T. S. Bergstedt, B. T. Hauser, and C. S. P. Cavalaheiro, *Langmuir* **16**, 795 (2000).
12. C. L. Exstrom, J. R. Sowa, C. A. Daws, D. Janzen, and K. R. Mann, *Chem. Mater.* **7**, 15 (1995).
13. L. X. Chen, W. J. H. Jager, D. J. Gosztola, M. P. Niemczyk, and M. R. Wasielewski, *J. Phys. Chem. B* **104**, 1950 (2000).
14. P. A. Buttry and A. J. Bard, (eds.), "Electroanalytical Chemistry." Marcel Dekker, Inc., New York, NY, (1991).
15. D. L. Feldheim, S. M. Hendrickson, M. Krejcik, C. M. Elliott, and C. A. Foss, *J. Phys. Chem.* **99**, 3288 (1995).